JACS
JOURNAL OF THE AMERICAN CHEMICAL SOCIETY

Communication

pubs.acs.org/JACS

A General Synthetic Approach for Ordered Mesoporous Metal Sulfides

Bryan T. Yonemoto, Gregory S. Hutchings, and Feng Jiao*

Center for Catalytic Science and Technology (CCST), Department of Chemical and Biomolecular Engineering, University of Delaware, Newark, Delaware 19716, United States

Supporting Information

ABSTRACT: Mesoporous non-silica materials have shown unique properties in many fields such as heterogeneous catalysis and energy conversion and storage. Many studies have been devoted to the synthesis of mesoporous transition-metal-containing materials. However, the range of materials that can be made is mainly limited to oxides. In this work, we developed an oxide-to-sulfide transformation approach as a general synthetic method to prepare ordered mesoporous metal sulfides. Three first-row transition-metal sulfides, FeS_2, CoS_2, and NiS_2, with highly ordered mesoporous structures and crystalline walls have been successfully synthesized for the first time. A preliminary investigation was performed to explore the photocatalytic properties of the newly synthesized mesoporous metal sulfides. All of the mesoporous metal sulfides exhibited higher activity than their bulk counterparts for the photocatalytic degradation of methylene blue dye under visible-light irradiation. More importantly, the preparation method introduced in this work may be extended to other mesoporous metal chalcogenides for a variety of potential applications.

Mesoporous materials have attracted attention because of their great potential as catalysts, electrodes, and magnetic materials.[1−7] Since the nanocasting method was introduced, a wide range of mesoporous transition-metal oxides, such as Fe_2O_3,[8,9] MnO_2,[10] Co_3O_4,[11,12] NiO,[13] and TiO_2,[14] with ordered pores and crystalline walls have been synthesized using mesoporous SBA-15[15] and KIT-6[16] silica as hard templates. Some unique behaviors of nanocast materials have been found for a number of applications.[17−19] For example, we recently synthesized a photocatalytically active ordered mesoporous Co_3O_4 with extremely high surface area by nanocasting a mesoporous $MgCo_2O_4$ and then selectively leaching the magnesium.[12,20] Through manipulation of the synthetic conditions and elemental compositions, the resulting Co_3O_4 material exhibited a much higher activity in the photocatalytic water oxidation reaction compared with its bulk counterpart. This study demonstrated the importance of synthesis in preparing mesoporous materials with the desired composition and porosity. To continue addressing critical challenges with mesoporous materials, new strategies to access materials that could not be synthesized previously are necessary.

Among all of the transition-metal-containing materials, metal sulfides are of particular interest because of their potential applications in sensors,[21] separations,[22] catalysis,[23] solar cells,[24,25] fuel cells,[26] and batteries.[27,28] A few attempts to synthesize mesoporous metal sulfides have been made.[21,22,29] Pioneering work by Gao et al.[30] showed the possibility of synthesizing ordered mesoporous metal sulfides via the nanocasting method. In the report of mesoporous WS_2 and MoS_2 by Shi et al.,[31] phosphotungstic acid ($H_3PW_{12}O_{40}\cdot 6H_2O$) and phosphomolybdic acid ($H_3PMo_{12}O_{40}\cdot 6H_2O$), respectively, were loaded into a mesoporous silica template and subjected to high-temperature thermal treatment (600 °C) under a flow of mixed H_2S and H_2. Although some important progress has been made, the range of ordered mesoporous metal sulfides that can be synthesized is still very limited.

A major challenge in the synthesis of mesoporous metal sulfides using the nanocasting method, as noted by Shi et al.,[31] is the large volume difference between the common metal precursors (i.e., nitrate salts) and the final product. In the case of iron, the unit cell volumes per iron atom in the precursor $Fe(NO_3)_3\cdot 9H_2O$ and the FeS_2 product are 372 and 40 Å^3/Fe, respectively. The 89% contraction in volume makes it very hard to form interconnected continuous-pore structures using traditional one-step nanocasting methods because the formed crystallites are likely to be isolated as small islands instead of interconnected networks. A recent study of container effects of nanocast metal oxides by Sun et al.[32] found that when a metal nitrate was used as the precursor, the metal oxides inside the silica template went through an acidic vapor dissolution−recrystallization process, resulting in the growth of large, interconnected, crystalline oxides within the porous silica template. Utilizing an analogous formation mechanism for metal sulfides is problematic because the thermodynamics of H_2S decomposition is not favorable at low temperatures[25,33] and the incompatibilities of H_2S and metal sulfides with strong oxidizers such as nitrates necessitate gas flow during synthesis. The gas flow drives away the aqueous vapors necessary for crystal growth via dissolution and reformation.

To circumvent this problem, we designed an "oxide-to-sulfide" strategy by first forming the metal oxide within the mesoporous silica template, taking advantage of the container effects to form well-ordered oxides, and then transforming the oxide to a sulfide through an H_2S/sulfur vapor treatment (Scheme 1). For example, in the case of iron, the metal atom

Received: May 2, 2014
Published: June 6, 2014

   dx.doi.org/10.1021/ja504407e | J. Am. Chem. Soc. 2014, 136, 8895−8898

Scheme 1. Oxide-to-Sulfide Transformation Can Be Used To Manage the Large Volume Contraction That Leads to Isolated Particles in a Traditional Nanocasting Procedure

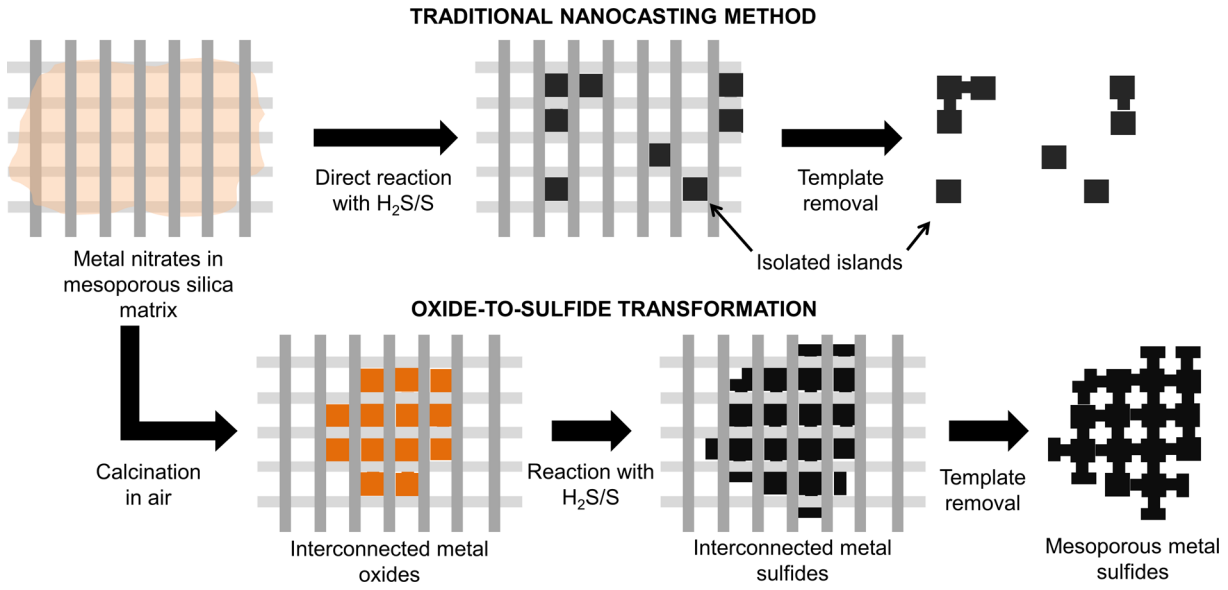

density in α-Fe_2O_3 is 25.2 Å^3/Fe, so the sulfidation conversion involves a much smaller, increasing volume change that ensures continued cohesiveness of the mesostructure within the hard template. Here we present the first synthesis of mesoporous iron sulfide, cobalt sulfide, and nickel sulfide with ordered pores and crystalline walls using the proposed oxide-to-sulfide nanocasting method. Preliminary photocatalytic studies confirmed that the mesoporous metal disulfides exhibit substantially better activities of methylene blue removal from water than their bulk counterparts.

Detailed synthetic procedures for the ordered mesoporous metal sulfides can be found in the Supporting Information. In the synthesis, we found that the reaction temperature is critical to form the desired mesostructure. A low reaction temperature (~250 °C) for the oxide-to-sulfide conversion in the mesoporous silica template is preferred, compared with the higher temperatures usually used for metal oxide to disulfide conversions (>375 °C).[24,25] At 390 °C, the iron sulfide system still produced an ordered mesoporous sample, while in the cases of cobalt and nickel, large particles of cobalt sulfide and nickel sulfide with poorly defined mesostructures were obtained as the dominant products. Another important step in the synthesis is the silica template removal. The 1.66 M NaOH aqueous solutions and deionized H_2O must be bubbled with N_2 to remove the dissolved oxygen before they are used; otherwise, low metal sulfide yields result because pyrite-phase materials dissolve in the presence of oxygen with redox-active metal cations in a basic environment.[34]

For the as-made mesoporous metal sulfides, we first examined the compositions of the resulting three mesoporous samples using energy-dispersive X-ray spectroscopy (EDS) because it is known that metal sulfide reactions are often off-stoichiometric.[35−37] On the basis of the EDS results, the estimated compositions for the as-synthesized samples are $Fe_{1.38}S_2$, $Co_{1.43}S_2$, and $Ni_{1.33}S_2$. Elemental mappings were also performed to confirm the uniform distribution of each element across the whole sample (Figure S1 in the Supporting Information).

Figure 1a,c,e shows typical transmission electron microscopy (TEM) images of the three as-made mesoporous metal sulfides. By checking many particles, we confirmed that ordered mesostructures are present in the iron sulfide, cobalt sulfide, and nickel sulfide materials, although some disordered particles were observed. High-resolution TEM (HRTEM) images (Figure 1b,d,f) show that lattice fringes are present within the crystalline walls, and the fringe distances are consistent with the metal disulfide crystallography. To further investigate the crystallinity and phase, wide-angle powder X-ray diffraction (PXRD) measurements were carried out. The results (Figure 2) show that the pyrite phase is the dominant crystal structure in all three samples. It should be noted that the PXRD pattern for the mesoporous iron sulfide sample (Figure 2b) shows some marcasite polymorph, which is very common for iron sulfide materials given their nearly identical densities.[24,27] Low-angle PXRD patterns for KIT-6 and all three mesoporous metal sulfides (Figure S2 in the Supporting Information) show a similar diffraction peak at ~1°, suggesting the existence of mesoscale order in all of the samples.

Gas adsorption studies confirmed the mesoporous nature of the nanocast metal sulfides. On the basis of the adsorption isotherms, a pore diameter of ~3.4 nm with a narrow size distribution was observed using the density functional theory method for all three metal sulfide samples (Figure S3 in the Supporting Information). This diameter is consistent with those of nanocast metal oxides from mesoporous KIT-6 silica templates.[13] The Brunauer−Emmett−Teller (BET) surface areas obtained from the N_2 adsorption measurements are 92, 86, and 77 $m^2\ g^{-1}$ for iron sulfide, cobalt sulfide, and nickel sulfide, respectively. The BET surface areas for metal sulfides are expected to be lower than those obtained for nanocast metal oxides (typically 100 $m^2\ g^{-1}$). This is due to the fact that the molecular weight per metal atom of a typical metal sulfide is higher than that of the corresponding oxide, resulting in less surface area per unit weight for materials with identical porosities. We estimated the equivalent surface areas if the molecular weights were those of the oxides instead of the sulfides, and the calculated values are very similar to the surface

dx.doi.org/10.1021/ja504407e | J. Am. Chem. Soc. 2014, 136, 8895−8898

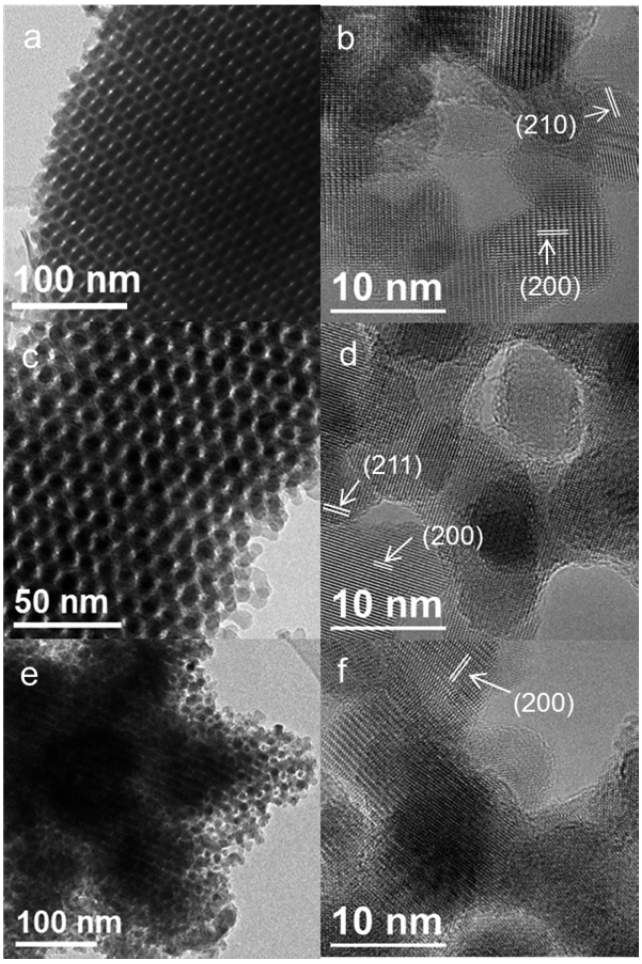

Figure 1. (a, c, e) TEM and (b, d, f) HRTEM images of (a, b) mesoporous iron sulfide, (c, d) mesoporous nickel sulfide, and (e, f) mesoporous cobalt sulfide materials.

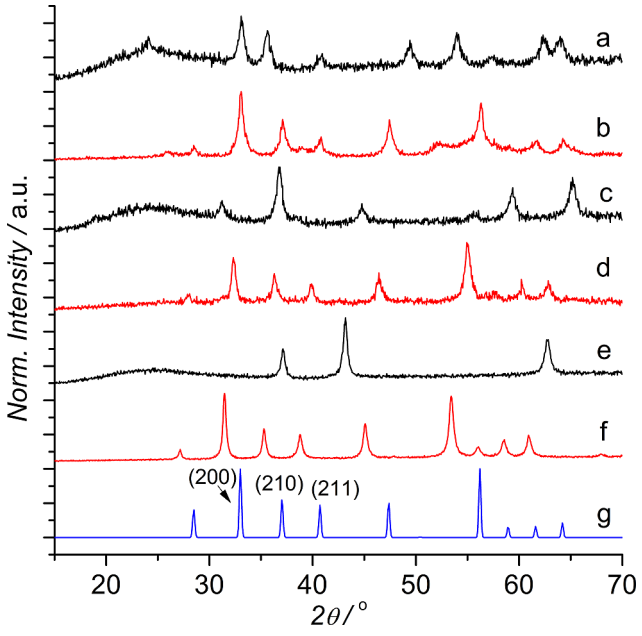

Figure 2. PXRD patterns for (a) Fe_2O_3 in KIT-6, (b) mesoporous iron sulfide, (c) Co_3O_4 in KIT-6, (d) mesoporous cobalt sulfide, (e) NiO in KIT-6, (f) mesoporous nickel sulfide, and (g) simulated pyrite FeS_2.

areas reported for nanocast metal oxides. A summary of the N_2 adsorption results (Table S1) and details of the calculation can be found in the Supporting Information. The appropriate surface area and pore diameter provide additional evidence of a successful oxide-to-sulfide transformation.

To demonstrate the improvements in performance possible with the new mesoporous metal sulfides, the simultaneous photocatalytic degradation and adsorption of a methylene blue solution was investigated. When only visible light and a very high methylene blue starting concentration of 32 mg/L were used, the mesoporous metal disulfides offered substantial improvements in methylene blue removal over nonporous catalysts with identical crystal structures (Figure 3). The low

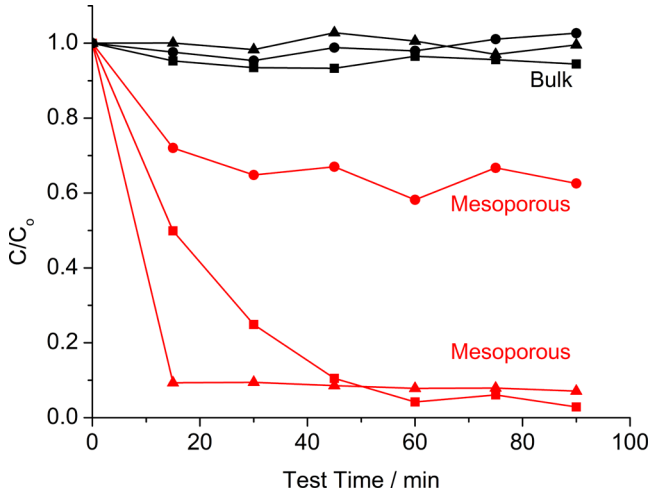

Figure 3. Adsorption with photocatalytic degradation of methylene blue by (red) mesoporous and (black) bulk FeS_2 (squares), CoS_2 (triangles), and NiS_2 (circles).

methylene blue removal of mesoporous NiS_2 compared with mesoporous FeS_2 and CoS_2 demonstrates that material composition plays an important role in the degradation reaction. We suspect that a surface phenomenon relating to the hydroxide anions formed during the photocatalytic degradation could account for the observed differences.[38,39] With a hydroxide ion at the surface, the metal site may need to change oxidation state from 2+ to 3+ to maintain charge neutrality. Nickel rarely oxidizes beyond 2+, so a cycle relying on an oxidative change, even if just momentarily, would be severely limited. Such a phenomenon was not observed in the cases of bulk metal sulfides, probably because their extremely low surface areas make the differences insignificant (Figure S3 in the Supporting Information).

In summary, we have developed an "oxide-to-sulfide" strategy and successfully synthesized the first examples of ordered mesoporous iron sulfide, nickel sulfide, and cobalt sulfide with crystalline walls. The excellent photocatalytic properties of mesoporous metal sulfides have been demonstrated via a methylene blue dye photodegradation reaction. The proposed synthetic strategy and novel metal sulfides reported in this paper will hopefully stimulate further investigations involving mesoporous sulfides for a variety of materials science applications.

dx.doi.org/10.1021/ja504407e | J. Am. Chem. Soc. 2014, 136, 8895−8898

■ ASSOCIATED CONTENT

Supporting Information

Experimental procedures, EDS elemental maps, low-angle and additional wide-angle PXRD patterns, and gas adsorption data. This material is available free of charge via the Internet at http://pubs.acs.org.

■ AUTHOR INFORMATION

Corresponding Author

jiao@udel.edu

Notes

The authors declare no competing financial interest.

■ ACKNOWLEDGMENTS

The authors acknowledge the financial support from the University of Delaware Research Foundation (UDRF). B.T.Y. was supported by a National Science Foundation Graduate Research Fellowship (Grant 0750966).

■ REFERENCES

(1) Yang, P. D.; Zhao, D. Y.; Margolese, D. I.; Chmelka, B. F.; Stucky, G. D. *Nature* **1998**, *396*, 152.
(2) Shi, Y.; Guo, B.; Corr, S. A.; Shi, Q.; Hu, Y.-S.; Heier, K. R.; Chen, L.; Seshadri, R.; Stucky, G. D. *Nano Lett.* **2009**, *9*, 4215.
(3) Poyraz, A. S.; Kuo, C.-H.; Biswas, S.; King'ondu, C. K.; Suib, S. L. *Nat. Commun.* **2013**, *4*, 2952.
(4) Deng, Y.; Qi, D.; Deng, C.; Zhang, X.; Zhao, D. *J. Am. Chem. Soc.* **2008**, *130*, 28.
(5) Tüysüz, H.; Lehmann, C. W.; Bongard, H.; Tesche, B.; Schmidt, R.; Schüth, F. *J. Am. Chem. Soc.* **2008**, *130*, 11510.
(6) Brezesinski, T.; Wang, J.; Tolbert, S. H.; Dunn, B. *Nat. Mater.* **2010**, *9*, 146.
(7) Lu, A.-H.; Schüth, F. *Adv. Mater.* **2006**, *18*, 1793.
(8) Jiao, F.; Harrison, A.; Jumas, J. C.; Chadwick, A. V.; Kockelmann, W.; Bruce, P. G. *J. Am. Chem. Soc.* **2006**, *128*, 5468.
(9) Jiao, F.; Yen, H. A.; Hutchings, G. S.; Yonemoto, B.; Lu, Q.; Kleitz, F. *J. Mater. Chem. A* **2014**, *2*, 3065.
(10) Ren, Y.; Ma, Z.; Morris, R. E.; Liu, Z.; Jiao, F.; Dai, S.; Bruce, P. G. *Nat. Commun.* **2013**, *4*, 2015.
(11) Rumplecker, A.; Kleitz, F.; Salabas, E.-L.; Schüth, F. *Chem. Mater.* **2007**, *19*, 485.
(12) Rosen, J.; Hutchings, G. S.; Jiao, F. *J. Am. Chem. Soc.* **2013**, *135*, 4516.
(13) Jiao, F.; Hill, A. H.; Harrison, A.; Berko, A.; Chadwick, A. V.; Bruce, P. G. *J. Am. Chem. Soc.* **2008**, *130*, 5262.
(14) Bian, Z.; Zhu, J.; Wen, J.; Cao, F.; Huo, Y.; Qian, X.; Cao, Y.; Shen, M.; Li, H.; Lu, Y. *Angew. Chem., Int. Ed.* **2011**, *50*, 1105.
(15) Zhao, D. Y.; Feng, J. L.; Huo, Q. S.; Melosh, N.; Fredrickson, G. H.; Chmelka, B. F.; Stucky, G. D. *Science* **1998**, *279*, 548.
(16) Kleitz, F.; Choi, S. H.; Ryoo, R. *Chem. Commun.* **2003**, 2136.
(17) Jiao, F.; Bruce, P. G. *Adv. Mater.* **2007**, *19*, 657.
(18) Yen, H.; Seo, Y.; Kaliaguine, S.; Kleitz, F. *Angew. Chem., Int. Ed.* **2012**, *51*, 12032.
(19) Crossland, E. J. W.; Noel, N.; Sivaram, V.; Leijtens, T.; Alexander-Webber, J. A.; Snaith, H. J. *Nature* **2013**, *495*, 215.
(20) Rosen, J.; Hutchings, G. S.; Jiao, F. *J. Catal.* **2014**, *310*, 2.
(21) Mohanan, J. L.; Arachchige, I. U.; Brock, S. L. *Science* **2005**, *307*, 397.
(22) Bag, S.; Trikalitis, P. N.; Chupas, P. J.; Armatas, G. S.; Kanatzidis, M. G. *Science* **2007**, *317*, 490.
(23) Kong, D.; Cha, J. J.; Wang, H.; Lee, H. R.; Cui, Y. *Energy Environ. Sci.* **2013**, *6*, 3553.
(24) Seefeld, S.; Limpinsel, M.; Liu, Y.; Farhi, N.; Weber, A.; Zhang, Y. N.; Berry, N.; Kwon, Y. J.; Perkins, C. L.; Hemminger, J. C.; Wu, R. Q.; Law, M. *J. Am. Chem. Soc.* **2013**, *135*, 4412.
(25) Morrish, R.; Silverstein, R.; Wolden, C. A. *J. Am. Chem. Soc.* **2012**, *134*, 17854.
(26) Wang, H.; Liang, Y.; Li, Y.; Dai, H. *Angew. Chem., Int. Ed.* **2011**, *50*, 10969.
(27) Shao-Horn, Y.; Osmialowski, S.; Horn, Q. C. *J. Electrochem. Soc.* **2002**, *149*, A1499.
(28) Hwang, H.; Kim, H.; Cho, J. *Nano Lett.* **2011**, *11*, 4826.
(29) Braun, P. V.; Osenar, P.; Tohver, V.; Kennedy, S. B.; Stupp, S. I. *J. Am. Chem. Soc.* **1999**, *121*, 7302.
(30) Gao, F.; Lu, Q. Y.; Zhao, D. Y. *Adv. Mater.* **2003**, *15*, 739.
(31) Shi, Y. F.; Wan, Y.; Liu, R. L.; Tu, B.; Zhao, D. Y. *J. Am. Chem. Soc.* **2007**, *129*, 9522.
(32) Sun, X.; Shi, Y.; Zhang, P.; Zheng, C.; Zheng, X.; Zhang, F.; Zhang, Y.; Guan, N.; Zhao, D.; Stucky, G. D. *J. Am. Chem. Soc.* **2011**, *133*, 14542.
(33) Wu, L. M.; Seo, D. K. *J. Am. Chem. Soc.* **2004**, *126*, 4676.
(34) Eggleston, C. M.; Ehrhardt, J. J.; Stumm, W. *Am. Mineral.* **1996**, *81*, 1036.
(35) Shao-Horn, Y.; Horn, Q. C. *Electrochim. Acta* **2001**, *46*, 2613.
(36) Mrowec, S.; Danielewski, M.; Wojtowicz, A. *J. Mater. Sci.* **1998**, *33*, 2617.
(37) Colson, J. C.; Gautherin, J. C.; Bert, P. *Mater. Res. Bull.* **1974**, *9*, 1447.
(38) Houas, A.; Lachheb, H.; Ksibi, M.; Elaloui, E.; Guillard, C.; Herrmann, J. M. *Appl. Catal., B* **2001**, *31*, 145.
(39) Wu, C.-H.; Chern, J.-M. *Ind. Eng. Chem. Res.* **2006**, *45*, 6450.